Sains Malaysiana 40(3)(2011): 237–244

Atomic Force Microscopy as a Tool for Asymmetric Polymeric Membrane Characterization

(Mikroskop Daya Atom sebagai Alat Pencirian Asimetrik Membran Polimer)

ABDUL WAHAB MOHAMMAD*, NIDAL HILAL, LIM YING PEI,
INDOK NURUL HASYIMAH MOHD AMIN & RAFEQAH RASLAN

ABSTRACT

Atomic force microscopy (AFM) has a wide range of applications and is rapidly growing in research and development. This powerful technique has been used to visualize surfaces both in liquid or gas media. It has been considered as an effective tool to investigate the surface structure for its ability to generate high-resolution 3D images at a subnanometer range without sample pretreatment. In this paper, the use of AFM to characterize the membrane roughness is presented for commercial and self-prepared membranes for specific applications. Surface roughness has been regarded as one of the most important surface properties, and has significant effect in membrane permeability and fouling behaviour. Several scan areas were used to compare surface roughness for different membrane samples. Characterization of the surfaces was achieved by measuring the average roughness (R_a) and root mean square roughness (R_{rms}) of the membrane. AFM image shows that the membrane surface was composed entirely of peaks and valleys. Surface roughness is substantially greater for commercial available hydrophobic membranes, in contrast to self-prepared membranes. This study also shows that foulants deposited on membrane surface would increase the membrane roughness.

Keywords: Atomic Force Microscopy (AFM); fouling; hydrophobic; membrane roughness

ABSTRAK

Mikroskop Daya Atom (AFM) mempunyai penggunaan yang meluas dan berkembang pesat dalam penyelidikan serta pembangunan. Teknik ini telah digunakan untuk menggambarkan permukaan di udara dan proses berkaitan persekitaran yang berair. Ia merupakan alat yang berkesan untuk menghasilkan imej 3D yang beresolusi tinggi struktur permukaan pada ukuran julat subnanometer tanpa penyediaan awal sampel. Dalam kajian ini, penggunaan Mikroskop Daya Atom untuk menentukan kekasaran membran ditunjukkan untuk membran komersial dan membran yang dihasilkan di makmal dan bagi aplikasi yang khusus. Kekasaran permukaan adalah salah satu ciri permukaan yang penting dan memberi kesan yang signifikan kepada kebolehtelapan air dan sifat kekotoran pada membran. Beberapa kawasan imbasan telah digunakan untuk memperbaiki perbezaan kekasaran permukaan pada sampel yang berlainan. Ciri-ciri permukaan telah diperolehi melalui ukuran purata kekasaran (R_a) dan punca kuasa dua kekasaran membran (R_{rms}). Imej AFM menunjukkan permukaaan membran terdiri daripada puncak dan lembah. Kekasaran permukaan adalah lebih tinggi bagi membran komersil sedia ada yang hidrofobik, berbeza dengan penghasilan membran sendiri. Kajian ini juga menunjukkan agen kotoran yang terendap pada permukaan membran akan meningkatkan kekasaran membran.

Kata kunci: Hidrofobik; kekasaran membran; kekotoran; Mikroskop Daya Atom (AFM)

INTRODUCTION

Membrane separation processes are one of the most important recent developments in the process industries and environmental protection. For optimum operation, the membrane has to possess physical properties giving appropriate interactions with solutes in the process stream. The most important of these properties are pores size distribution, surface morphology, appropriate long range electrostatic interactions and the minimum attachment of solutes to the membrane surface (Park et al. 2005). However, for practical processes the deposition of solutes or dispersed materials on the membrane surface, membrane fouling, is an inevitable phenomenon, even with pretreatment, optimum system design and/or excellent anti-fouled membrane properties. Membrane fouling causes flux decline and frequent membrane cleaning/replacement reduce the efficiency and economic benefits of membrane processes. Thus, understanding the relationship of polymer-membrane-surface properties to fouling processes is of great interest to improve fouling prevention technique. Measurements at the nanoscale which incorporate the effects of surface morphology are therefore needed. AFM technique is capable of such measurements.

Atomic Force Microscopy (AFM) can produce topographical images by scanning a microscopic tip at the end of a cantilever over a surface. The technique has been

used to produce images of many materials and resolution can reach atomic dimensions for flat surfaces (Bessieres et al. 1996). Uniquely, AFM can image surfaces in air or in liquid without any special sample preparation. The technique has been applied to the study of membranes (Bowen & Doneva 2000) yielding information on surface morphology, surface porosity, and the dimensions of adsorbed agglomerates (Bowen et al. 1998a). Early applications of atomic force microscopy to membrane separation processes have been carried out by Bowen et al. (1999a). Other researchers used atomic force microscopy to investigate microfiltration and ultrafiltration membrane surface structures (Bottino et al. 1994; Chahboun et al. 1992; Dietz et al. 1992; Miwa et al. 1992) and to elucidate the mechanisms giving rise to fouling in membrane processing (Bowen 1993). Another key feature of AFM is its ability to measure force interactions as a function of probe-surface separation distance (Ducker et al. 1992). The technique used involves the immobilization of a particle at the end of the cantilever, creating a "colloid probe". The technique has been used to quantify adhesion of polymeric latex particles, biological cells, and proteins to smooth ultrafiltration membranes (Bowen et al. 1998b, 1999c). Such measurements allow an assessment of the fouling propensity of membranes without the need of process measurements. The fundamental AFM study of membranes has been applied further in the development of new polymer blend membranes of promising properties: high permeability and low adhesion (Chahboun et al. 1992).

An important advantage of AFM in the study of surface properties, including membrane, is the ability to quantify both surface morphology and surface interactions with a single instrument. For example, by scanning a colloid probe over a microfiltration membrane surface it was possible to visualize and quantify the importance of electrical double-layer interactions on the separation of particles by pores in such membranes (Bowen et al. 1999b). In the context of particle adhesion at surfaces, of which membrane fouling in an important technological example, surface roughness is an important parameter (Mizes 1995; Walz 1998). The aim of the present study is to characterize ultrafiltration membrane surface roughness using the AFM technique and to correlate this data to membrane process performance. Both self-prepared and commercial membranes have been used.

MATERIALS AND METHOD

MATERIALS

Case study I: Preparation of Polysulfone/ Pluronic F127 Blend Membrane Polysulfone/Pluronic F127 membranes were prepared by phase inversion method. The formulations of casting solution are given in Table 1. Polysulfone was a membrane matrix whereas Pluronic F127 was a membrane modifier as well as a pore-forming agent. Polysulfone and various amount of Pluronic F127 were dissolved in NMP and stirred at 80°C for about 4 hours to obtain homogeneous mixing and then left for overnight to allow complete release of bubbles. The solutions were then cast on glass plates with a filmographe doctor blade (Braive Instrument), and then immersed in a coagulation bath of deionized water. Subsequently, the membranes formed were peeled off and washed thoroughly with deionized water to remove any residual solvent. The prepared membranes were kept in deionized water before testing.

Case study II: Ultrafiltration Membrane Fouled by Gelatin Two different type of membrane materials, namely, polyethersulfone and regenerated cellulose acetate of 30 kDa molecular weight cut-off (MWCO) were tested. The physical properties of the membrane are shown in Table 2. Each of the membrane disks was soaked for 24 hours overnight at room temperature in deionized water before being used. The clean membrane hydraulic permeability (L_{po}) was calculated for each membrane sample according to Darcy's Law (Pagliero et al. 2001):

$$L_P = \frac{J_V}{\Delta P}, \tag{1}$$

where L_p, J_v and ΔP are hydraulic permeability [L/(m^2 h bar)], water flux (L/m^2 h) and transmembrane pressure (bar), repectively. Gelatin of pharmaceutical grade from Halagel (M) Sdn Bhd with means molecular weight of 188 kDa and isoelectric point (IEP) of 5.04 was used as model protein. The experiments were carried out by using a dead-end stirred cell filtration system (Amicon cell models 8200) from Millipore Co., USA with a volume capacity of 200 mL. All experiments were carried out at 40°C, above the gelling point of gelatine, around 33°C. Each membrane was initially compacted before use by filtering pure water at 2.5 bar for at least 30 min. The stirred cell was then

TABLE 1. The formation of casting solutions for preparation of the polysulfone/pluronic F127 membranes

Membrane	PSU (g)	Pluronic F127 (g)	NMP (g)	$W_{F127}/W_{total\ polymer}$ (%)
P-0	14.16	-	51.40	0
P-30	9.91	4.25	51.40	30

emptied and refilled with 40 g/L protein solution and the outer membrane surface was exposed for a period of time with no pressure applied at a stirring rate of 500 rpm. Thereafter, the solution was removed, and the membrane surface was rinsed two times by filling the cell with pure water (100 mL) and shaking it for 30 s. Pure water flux was measured again and membrane permeability after adsorption (L_{pa}) was recalculated afterwards.

Case study III: Ultrafiltration Membrane Fouled by Palm Oil Based Fatty Acids Oleic, stearic and palmitic acid were purchased from Merck, and used as co-foulant model in the study, while glycerin was provided from Sigma and meets the USP testing. The molar masses of palmitic acid 256.42 g/mol, stearic acid 284.48 g/mol, oleic acid 282.46 g/mol and glycerin at 92.09 g/mol, used as received. Glycerin-water mixtures with different types of fatty acids were prepared and the compositions of fatty acids in the mixture were based on their maximum solubility in pure water, as shown in Table 3. The fatty acid was initially dissolved in one liter of pure water prior to mix with glycerin. Ultrafiltration flat sheet polymeric membranes made of PES, obtained from Sterlitech Corporation, was used in the fouling experiments. The properties of the membrane are shown in the Table 2. All the new membranes soaked in pure water overnight prior to each run, then removed and rinsed with pure water once the experiment completed.

METHODS

All AFM measurements were carried out using multimode AFM with a Nanoscope IIIa controller (Veeco, Santa Barbara CA) and contact mode OTR8 silicon nitride probes (Olympus, Japan). Prior to the measurements, the probes were cleaned in argon plasma. Membrane samples were attached to the metal sample discs using epoxy resin. Measurements were all carried out under ambient conditions using the contact mode of imaging. Roughness parameters were extracted from AFM topography using instrument's software. Surfaces can be compared in terms of roughness parameters, such as the mean roughness R_a (nm), mean square of the Z data R_q (nm), and mean difference in height between the highest peaks and five lowest valleys R_z (nm), as well as in terms of the diameter of the nodules. $\tilde{Z}$ is defined as the difference between the highest and lowest points within the given area (nm). The roughness parameters depend on the curvature and the size of the TM-AFM tip, as well as on the treatment of the captured surface data (plane fitting, flattering, filtering, etc.). Therefore, the roughness parameters should not be considered as absolute roughness values. The mean roughness is the mean value of the surface relative to the center plane, the plane for which the volumes enclosed by the image above and below this plane are equal, and is calculated as:

$$Ra = \frac{1}{L_x L_y} \int_0^{L_y} \int_0^{L_x} |f(x,y)| dxdy, \tag{2}$$

where $f(x,y)$ is the surface relative to the central plane and L_x and L_y are the dimensions of the surface. The root mean square (rms) roughness parameter is a statistical measure of the relative roughness of a surface and is essentially the standard deviation of the heights for all the pixels in the image from the arithmetic mean, and can be summarised by:

$$rms = \sqrt{\frac{\sum (Z_i - Z_{ave})^2}{N}}, \tag{3}$$

where Z_i is the height value for a particular point on the image (nm), Z_{ave} is the mean height of all the pixels in the image (nm) and N is the total number of pixels within the image. The maximum range is the height difference between the lowest and highest pixels in the image.

TABLE 2. Properties of membranes

Membrane	Manufacturer	Material	MWCO (Da)	Contact angle, θ	Surface property
RCA 30	Millipore	Regenerated Cellulose Acetate	30 000	12	Hydrophilic
PES 30	Millipore	Polyethersulphone	30 000	65	Hydrophobic
PES25	Koch	Polyethersulphone	25 000	62.67	Hydrophobic

TABLE 3. Properties of fatty acids and glycerin

Solutes	Formula	MW (g/mol)	Solubility (g/L)
Palmitic acid	$C_{16:0}$	256.42	0.007
Stearic acid	$C_{18:0}$	284.48	0.089
Oleic acid	$C_{18:1}$	282.46	0.003
Glycerin	$C_{3:0}$	92.09	Soluble

Results and Discussion

Case study I: Preparation of Polysulfone/ Pluronic F127 Blend Membrane The data for roughness parameters, R_a and R_{rms} for P-0 and P-30 at at three different scan areas of (50 μm × 50μm), (25 μm × 25μm) and (5 μm × 5 μm) are presented in Table 4. Several scan areas were used in order to improve comparison of surface roughness for the different samples (Boussu et al. 2006). It can be seen that the roughness varied with the scanned areas which follows the trend, the larger the scanned area, the rougher the membrane. This proved that scanned area demonstrates an important role, as described by other authors (Boussu et al. 2005; Hilal et al. 2004; Veríssimo et al. 2006). According to Boussu et al. (2005) and Boussu et al. (2006), the trend of increasing roughness with increasing scan area can be related to the dependency of the roughness on the spatial wavelength of the scanned area or the frequency. For a small surface area, only the roughness of the "higher" frequencies is measured. When a larger surface area is scanned the roughness caused by additional lower frequencies also has to be taken into account. This results in a larger roughness value when a larger surface area is scanned. Another explanation for the increasing roughness with increasing scan size may be the formation of a fractal structure on the membrane surface when polymers are assembled to nodules or aggregates of nodules. So, when the scan size is changed, it is possible to get a different surface topography, resulting in a different roughness. Therefore, it is crucial that the same scan size range is used when comparing the surface roughness for different samples.

The roughness parameter for P-30 was obviously higher than P-0 at three different scanned areas. Lin et al. (2009) also claimed that the higher the Pluronic F127 content, the larger the roughness is. In order to visualize the difference in roughness, AFM images of P-0 and P-30 on a scan area of (5 μm × 5 μm) are presented in Figure 1 and 2, respectively. As can be seen in Figure 2, P-30 is lighter than P-0 which indicates a rougher membrane.

Case study II: Ultrafiltration Membrane Fouled by Gelatin Two UF membranes which are different in hydrophilicity properties were used in this study, as depicted in Figures 3 and 5, respectively. A hydrophilic regenerated cellulose acetate (RCA) and hydrophobic polyethersulfone (PES) of 30 kDa were placed in contact with gelatin solution in static mode. The average roughness and root mean square roughness of the clean and fouled by gelatin are shown in Table 5. It can be seen that both membranes become rougher after adsorption study due to the formation of foulant layer (gelatin) on the membrane surface, whose presence is confirmed by AFM images (Figures 4 and 6). In addition, it has been previously reported that adhesive force is larger for membranes with higher roughness compared to the smooth membranes (Bowen et al. 1998b). It is shown from Table 5 that PES has the higher value of roughness compared to RCA. This means that this membrane is expected to have relatively high adhesive force and

TABLE 4. Roughness measurement of P-0 and P-30

Surface Roughness (size scanned area)	Membranes	
	P-0	P-30
R_a (50 μm × 50μm)	13.519	47.045
R_a (25 μm × 25μm)	10.464	33.588
R_a (5 μm × 5μm)	2.575	3.981
R_{rms} (50 μm × 50 μm)	24.268	60.264
R_{rms} (25 μm × 25 μm)	16.673	44.014
R_{rms} (5 μm × 5 μm)	3.302	5.102

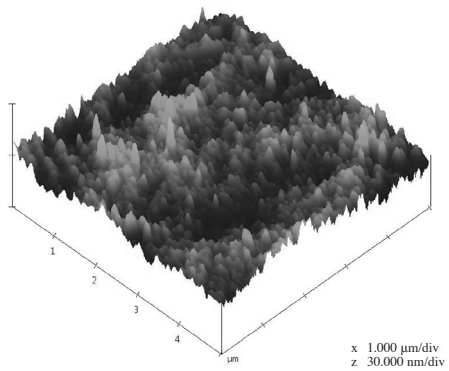

FIGURE 1. P-0 membrane

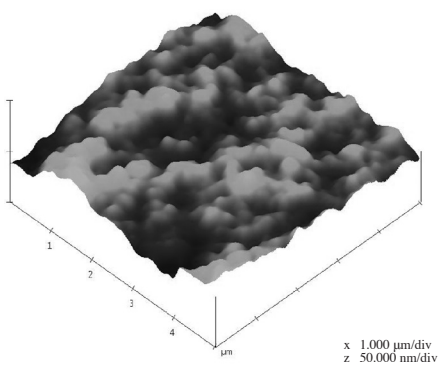

FIGURE 2. P-30 membrane

TABLE 5. Roughness measurement of RCA and PES membrane by fouled by gelatin

Surface Rougness (sized scanned area)	Membranes			
	RCA Clean	RCA Fouled	PES Clean	PES Fouled
R_a (25 μm × 25 μm)	3.804	24.001	8.529	42.228
R_a (5 μm × 5 μm)	1.274	5.34	3.853	9.827
R_a (1 μm × 1 μm)	0.742	2.052	0.992	2.271
R_{rms} (25 μm × 25 μm)	5.415	45.259	11.003	62.543
R_{rms} (5 μm × 5 μm)	1.713	6.877	5.285	12.776
R_{rms} (1 μm × 1 μm)	0.963	2.569	1.333	2.960

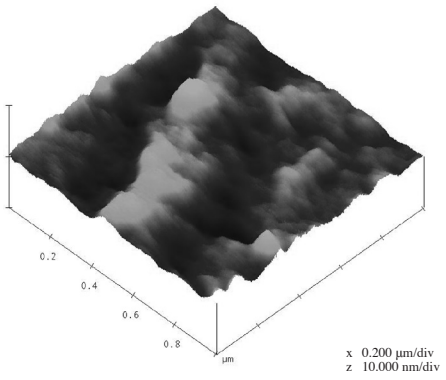

FIGURE 3. Clean RCA membrane

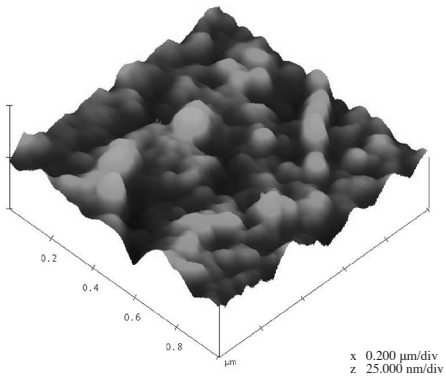

FIGURE 4. RCA membrane fouled by protein

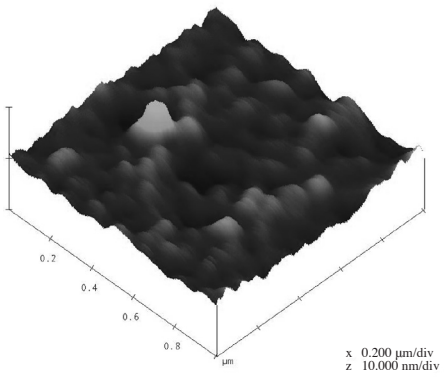

FIGURE 5. Clean PES membrane

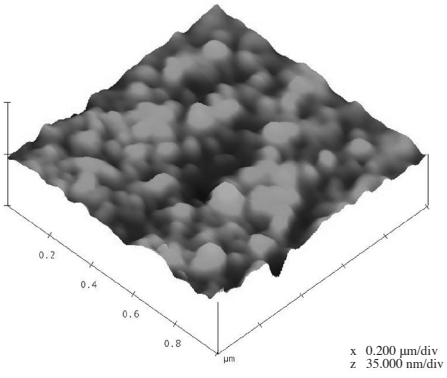

FIGURE 6. PES membrane fouled by protein

resulting in high fouling on its surface. This observation could be due to the membrane material (regenerated cellulose acetate) which is totally ionic and contains no a polar regions to bind protein by hydrophobic interaction. In contrast, when gelatin is exposed to a hydrophobic membrane surface, it hydrophilic outside exposed to the aqueous medium and the hydrophobic part adhering to the membrane. This result agreed well with the relative flux reduction, RFR results which showed 5 – 10% for RCA membrane, in contrast to 75% by PES membrane.

Case study III: Ultrafiltration Membrane Fouled by Palm Oil Based Fatty Acids A flat-sheet UF PES membrane was used to investigate the effect of each fatty acid on the fouling behavior and analyzed using an atomic force microscopy. Figure 7 to 10 depict the three dimensional AFM images of fresh PES membranes and those fouled with fatty acids. It is clearly shown that fresh PES membranes exhibited the major dark spots, indicating the rougher surface and contained large number of pores. It is also interesting to note that the PES membrane fouled with oleic and stearic acid exhibited the major bright spots, indicating more solutes adsorbing on the surface, therefore, lead to severe fouling in comparison with palmitic acid. It is probably due to the fact that both of oleic and stearic acid owing the longest hydrocarbon chain compared to palmitic acid. According to Jonsson et al. (1997), the thickness of adsorbed layer on the membrane surface corresponds to

the chain length of the molecule. Nevertheless, according to Figures 8 and 9, oleic acid revealed the brighter spot than stearic acid even though they were having equal carbon number (CN). However, the existence of cis-group in oleic acid will formed a V-shape in the middle of the chain, thus facilitating the fatty acid to be folded and block the membrane pores. Moreover, the data in Figure 8 revealed that most of the nodules (represents by brighter peaks) are merging each other and formed aggregation, which results to higher separation in comparison to data in Figure 9. Apparently, it probably explained severe fouling caused by oleic acid and lead to higher roughness (R_a) which is shown in Table 6. The data in Figure 10 depicts that the brighter spots blocked the darker one (represents the membrane pores), and results to pore blocking by palmitic acid. Hence, the PES membrane is less susceptible to fouling caused by palmitic acid and this statement support the roughness value which represented in Table 6. The roughness of the fouled PES membrane was found to increase with the increasing scanning area (Table 6) as well as influenced by the carbon chain length of each fatty acid. It is noted that the R_a values increased from 2.654 to 14.064 nm for fresh membrane due to the greater scan area. It might be explained by its dependency to the frequency and wavelength of the scanned area. A similar trend can be found for the fouled PES membrane which is attributed to the scan area.

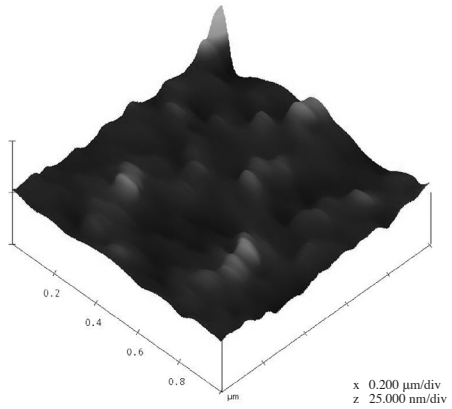

FIGURE 7. Clean PES membrane

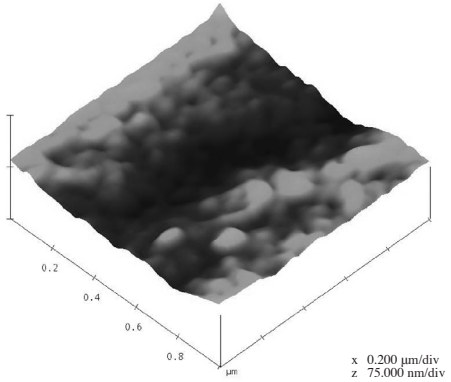

FIGURE 8. PES-fouled-oleic acid

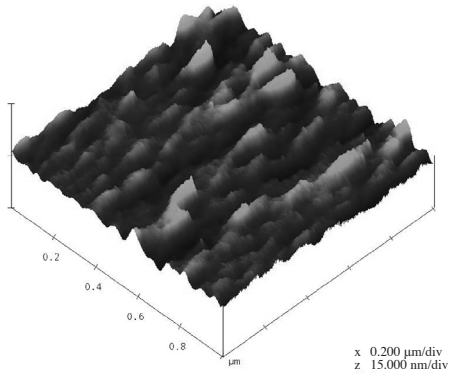

FIGURE 9. PES-fouled-stearic acid

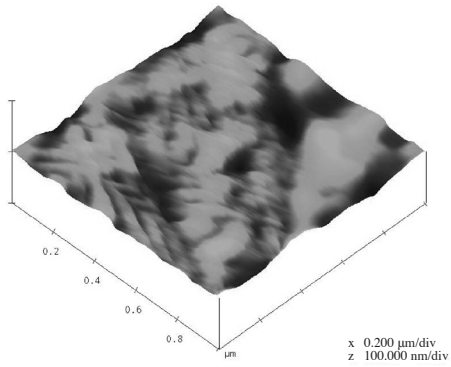

FIGURE 10. PES-fouled-palmitic acid

TABLE 6. Roughness measurement of PES membrane fouled by fatty acids

Surface Roughness (sized scanned area)	Membranes			
	PES Clean	PES Fouled-oleic	PES Fouled-palmitic	PES Fouled-stearic
R_a (25 µm × 25 µm)	14.064	78.424	92.145	73.350
R_a (5 µm × 5 µm)	8.781	35.173	57.518	48.439
R_a (1 µm × 1 µm)	2.654	8.597	7.474	8.524
R_{rms} (25 µm × 25 µm)	21.866	120.187	152.200	98.572
R_{rms} (5 µm × 5 µm)	18.391	45.595	75.811	65.361
R_{rms} (1 µm × 1 µm)	6.402	11.163	9.596	10.900

CONCLUSION

AFM has been proven to be one of the effective instrument to indicate the extent of surface properties of various hydrophobic polymer membranes of both the commercially available and self-prepared blend membranes. The key findings in this study are:

1. The presence of Pluronic F127 in the self-prepared blend membranes increase the membrane surface roughness. The overall changes in surface roughness, either in membrane surface modification or in contact with industrial feed stream, may be used as an indicator of a membrane's tendency to foul during filtration at given conditions. In the future, it should be possible to apply this technique to different types of membranes for fouling susceptibility of different process streams assessment.
2. The surface roughness for commercially available hydrophobic membranes were higher compared to hydrophilic membranes, thus fouling potential were more pronounced in proteinase solution and fatty acids with higher carbon number

ACKNOWLEDGEMENTS

This work has been supported by Universiti Kebangsaan Malaysia via grant UKM-GUP-KPB-08-32-129 and Malaysian Ministry of Science and Technology via TechnoFund TF0206A084.

REFERENCES

Bessieres, A., Meireles, M., Coratger, R. & Sanchez, J.B.V. 1996. Investigations of surface properties of polymeric membranes by near field microscopy. *Journal of Membrane Science* 109: 271-284.

Bottino, A., Capannelli, G., Grosso, A., Monticelli, O., Cavalleri, O., Rolandi, R. & Soria, R. 1994. Surface characterization of ceramic membranes by atomic force microscopy. *Journal of Membrane Science* 95: 289-296.

Boussu, K., Van der Bruggen, B., Volodin, A., Snauwaert, J., Van Haesendock, C. & Vandecasteele, C. 2005. Roughness and hydrophobicity studies of nanofiltration membranes using different modes of AFM. *Journal of Colloid and Interface Science* 286: 632-638.

Boussu, K., Van der Bruggen, B., Volodin, A., Van Haesendonck, C., Delcour, J.A., Van der Meeren, P. & Vandecasteele, C. 2006. Characterization of commercial nanofiltration membranes and comparison with self-made polyethersulfone membranes. *Desalination* 191: 245-253.

Bowen, W.R. 1993. In *Membranes in Bioprocessing*, edited by Howell, J.A., Sanchez, V. & Field, R.W. 265-291. London: Blackie.

Bowen, W.R. & Doneva, T.A. 2000. Artefacts in AFM studies of membranes: correcting pore images using fast fourier transform filtering. *Journal of Membrane Science* 171: 141-147.

Bowen, W.R., Hilal, N., Lovitt, R.W. & Wright, C.J. 1998a. Atomic force microscopy as a tool for the membrane technologist. *Microscopy and Analysis* 68: 13-16.

Bowen, W.R., Hilal, N., Lovitt, R.W. & Wright, C.J. 1998b, A new technique for membrane characterisation: Direct measurement of the force of adhesion of a single particle using an atomic force microscope. *Journal of Membrane Science* 139: 269-274.

Bowen, W.R., Hilal, N., Lovitt, R.W. & Wright, C.J. 1999a. Atomic force microscope studies of membrane surfaces, In *Surface Chemistry and Electrochemistry of Membrane Surfaces*, edited by Sørensen, T.S. (ed.). *Surfactant Science Series* 79: 1-37.

Bowen, W.R., Hilal, N., Jain, M., Lovitt, R.W., Sharif, A.O. & Wright, C.J. 1999b. The effects of electrostatic interactions on the rejection of colloids by membrane pores – visualization and quantification. *Chemical Engineering Science* 54: 369-375.

Bowen, W.R., Hilal, N., Lovitt, R.W. & Wright, C.J., 1999c. Characterisation of membrane surfaces: Direct measurement of biological adhesion using an atomic force microscope. *Journal of Membrane Science* 154: 205-212.

Chahboun, A., Coratger, R., Ajustron, F., Beauvillian, J., Aimar, P. & Sanchez, V. 1992. Comparative study of micro– and ultrafiltration membranes using STM, AFM and SEM techniques. *Ultramicroscopy* 41: 235-244.

Dietz, P., Hansma, P.K., Inacker, O., Lehmann, H.D. & Herrmann, K.H. 1992. Surface pore structures of micro- and ultrafiltration membranes imaged with the atomic force microscope. *Journal of Membrane Science* 65: 101-111.

Ducker, W.A., Senden T. J. & Pashley, R.M. 1992. Measurements of forces in liquids using a force microscope. *Langmuir* 8: 1831-1836.

Hilal, N., Al-Zoubi, H., Darwish, N.A., Mohammad, A.W. & Abu Arabi, M. 2004. A comprehensive review of nanofiltration membranes: Treatment, pretreatment, modelling, and atomic force microscopy. *Desalination* 170: 281-308.

Jönsson, A.S., Lindau, J., Wimmerstedt, R., Brinck, J. & Jönsson, B. 1997. Influence of the concentration of a low-molecular organic solute on the flux reduction of a polyethersulphone ultrafiltration membrane. *Journal of Membrane Science* 135: 117-128.

Lin, C.H., Lin, W.C. & Yang, M.C. 2009. Fabrication and characterization of ophthalmically compatible hydrogels composed of poly(dimethyl siloxane-urethane)/Pluronic F127. *Colloids and Surfaces B: Biointerfaces* 71: 36-44.

Miwa, T., Yamaki, M., Yoshimusa, H., Ebina, S. & Nagayama, K. 1992. Artifacts in atomic force microscopy images of fine particle and protein two-dimensional crystals as evaluated with scanning electron microscopy and simulations. *Japanese Journal of Applied Physics* 31: L1495.

Mizes, H.A. 1995. Surface Roughness and Particle Adhesion. *The Journal of Adhesion* 51: 155-165.

Pagliero, C., Ochoa, N., Marchese, J. & Mattea, M. 2001. Degumming of crude soybean oil by ultrafiltration using polymeric membranes. *Journal of the American Oil Chemists' Society* 78: 793-796.

Park, N., Kwon, B., Kim, I.S. & Cho, J.W. 2005. Biofouling potential of various NF membranes with respect to bacteria and their soluble microbial products (SMP): Characterizations, flux decline, and transport parameters. *Journal of Membrane Science* 258: 43-54.

Veríssimo, S., Peinemann, K.V. & Bordado, J. 2006. Influence of the diamine structure on the nanofiltration performance, surface morphology and surface charge of the composite polyamide membranes. *Journal of Membrane Science* 279: 266-275.

Walz, J.Y. 1998. The effect of surface heterogeneities on colloidal forces. *Advances in Colloid and Interface Science* 74: 119-168.

Abdul Wahab Mohammad*, Lim Ying Pei, Indok Nurul Hasyimah Mohd Amin & Rafeqah Raslan
Department of Chemical and Process Engineering
Faculty of Engineering and Built Environment
Universiti Kebangsaan Malaysia
43600 UKM Bangi, Selangor D.E.
Malaysia

Nidal Hilal
Centre for Water Advanced Technologies and Environmental Research (CWATER)
Multidisciplinary Nanotechnology Centre
College of Engineering
Swansea University
Swansea SA2 8PP
United Kingdom

Corresponding author; e-mail: wahabm@vlsi.eng.ukm.my

Received: 15 July 2010
Accepted: 3 September 2010